

## Structure and corrosion resistance of Ni-P, Co-P and Ni-Co-P alloy coatings

K. N. Ignatova<sup>1\*</sup>, St. V. Kozhukharov<sup>1</sup>, G. V. Avdeev<sup>2</sup>, I. A. Piroeva<sup>2</sup>

<sup>1</sup> University of Chemical Technology and Metallurgy – 8, Kl. Ohridski Blvd, Sofia 1756, Bulgaria

<sup>2</sup> Bulgarian Academy of Sciences, Institute of Physical Chemistry “Acad. Rostislav Kaishev”, Acad. G. Bonchev” St., Bl.11, Sofia 1113, Bulgaria

Received August 21, 2014; Accepted November 07, 2017

The present research work reports the results acquired from the systematical characterization regarding the morphology, the phase composition, the barrier properties and the corrosion resistance, possessed by Ni-P, Co-P and Ni-Co-P coatings on copper substrates. The investigated coatings were galvanostatically deposited at similar conditions from sulfate-chloride electrolytes, with pH = 2, at 80°C. The XRD analysis results have revealed that the Ni-P alloy coating possesses typically amorphous structure, whereas the Co-P coatings are with homogeneous polycrystalline structures, composed by orthorhombic Co<sub>2</sub>P phase. The Ni-Co-P coating has nano-sized structure and possesses variable composition consisted by series of solid solution Ni<sub>2</sub>P-Co<sub>2</sub>P depending on the content of the main elements. The results obtained from Electrochemical Impedance Spectroscopy (EIS) and Linear Sweep Voltammetry (LSV) for the barrier ability and the corrosion durability reveal clear correlation between themselves. The quantitative data acquired by both EIS and LVA methods applied during exposure from 24 to 672 hours to 3.5% NaCl have shown that the superior corrosion protective characteristics belong to the Ni-Co-P three-component layer. Besides, both Ni-Co-P and Ni-P alloy coatings preserve their barrier properties during the entire 672 h exposure cycle. For comparison, the Co-P coating was completely broken after 168 hours of exposure to the model corrosive medium.

**Key words:** nickel-cobalt-phosphorus coatings, morphology, phase composition, corrosion resistance, impedance analysis

### INTRODUCTION

The Ni-P based alloy coatings are being largely used in various industrial branches due to their significant mechanical strength, low friction coefficient, and remarkable durability in corrosive media [1, 2]. The main application fields of these coatings are the automobile and the aircraft industry [2]. Furthermore, these materials are used as electrocatalytic material for hydrogen production by water splitting [3]. The Co-P based compositions are also interesting for potential industrial application, because of their superplastic extensibility [4], superior wear resistance [5, 6], high saturation magnetization and considerable thermal stability [7, 8].

Recently, the Ni-Co-P ternary alloyed coatings became object of intensive research activities [9, 10], because these compositions combine the extended protective capabilities, typical for Ni-P alloys and the specific tribological and magnetic properties owed by the cobalt enriched Co-Ni based materials [9]. In addition, the ternary alloys with 70% of Ni content (15-20%Co, 10-15%P), appear to be a promising alternative of the hard chromate coatings [11, 12].

The electrochemical deposition of all the three types of Ni-P, Co-P and Ni-Co-P coatings could be performed from sulphate [13], modified Watts [10, 14, 15], chloride [14], citrate [16] and sulfamate [2] electrolytes on copper or low carbon steel substrates, predominantly at high temperatures (80-90°C). The correlation between the component composition, the morphological and structural features, possessed by Ni-P, Co-P and Ni-Co-P films by one side, and their resulting protective abilities on the other side, was object of various researchers [1, 6, 10, 13]. Parente [10] has performed an extended research on the thermal treatment impact on the corrosion protective ability of Ni-P and Ni-Co-P, by systematical EIS and LSV measurements. According to various authors [10, 17, 18], the amorphous state enhances the durability of these coatings against corrosion attack. Moreover, the amorphisation in these cases is favoured by the increase of phosphorous content from 7 to 10% [9, 10, 17]. The superior corrosion protective abilities of the amorphous alloys can be explained by the lower interatomic distances (i.e. closed structural packaging), resulting in low density of grain boundaries, dislocations and other surface

\* To whom all correspondence should be sent.  
E-mail: katya59ignatova@gmail.com

defects [9, 17]. In this sense, the comparison of Ni-P, Co-P and Ni-Co-P alloy films, deposited at identical conditions (i.e. current density, temperature, pH, etc.) appears as an actual task of considerable interest. Its decision should enable to clarify the role of each coating ingredient on the corrosion protective ability of the resulting ternary Ni-Co-P composition.

The present research aims to compare the characteristics of Ni-P, Co-P and Ni-Co-P, deposited on copper substrates from sulfate-chloride electrolyte, at identical conditions. For this purpose, inherent phase composition, morphology, as well as the resulting barrier ability and durability against corrosion were submitted to elucidation and further analysis.

### EXPERIMENTAL

The deposition kinetics was studied in three-electrode electrochemical cell with 150 dm<sup>3</sup> of volume at thermostatic conditions (80°C). The

working electrode was copper (MERK, 99.97%) disc with surface area of 1 cm<sup>2</sup>, insulated by epoxide rubber in plexiglass holder. The counter electrode was a platinum sheet with at least ten times larger surface area. The potentiostatic recording of the polarization dependencies was performed with saturated calomel electrode ( $E_{SCE} = 0.241 \div 0.244$  V) as reference, placed in a separate space connected to the cell by Lugin capillary.

The depositions were done in two electrode configuration cell against a platinum electrode in galvanostatic regime for 40 min. at current density of 65 mA cm<sup>-2</sup> on copper foil (MERK, 99.97%) electrodes with 2x2 cm of size (4 cm<sup>2</sup>). Ni-P, Co-P and Ni-Co-P alloy deposits were obtained by electrodeposition from solution with a similar composition as in [10] at 80°C, but by replacement of the H<sub>3</sub>PO<sub>4</sub> with H<sub>3</sub>PO<sub>3</sub> (Table 1) and in the absence of Na<sub>2</sub>CO<sub>3</sub>, which makes the solution more stable.

**Table 1.** Basic electrolytes composition (pH = 2)

Coating type	Electrolyte content (in [gmol dm <sup>-3</sup> ])				
	NiSO <sub>4</sub> .6H <sub>2</sub> O	NiCl <sub>2</sub> .H <sub>2</sub> O	CoSO <sub>4</sub> .7H <sub>2</sub> O	NaH <sub>2</sub> PO <sub>2</sub>	H <sub>3</sub> PO <sub>3</sub>
<b>Ni-P</b>	0.66	0.20	-----	0.60	0.60
<b>Co-P</b>	-----	-----	0.35	0.60	0.60
<b>Ni-Co-P</b>	0.66	0.20	0.35	0.60	0.60

The respective pH values (pH ≈ 2) were corrected by diluted NaOH or H<sub>2</sub>SO<sub>4</sub> aqueous solutions. Immediately prior to these electrochemical procedures, the copper substrates were always submitted to cleaning procedures involving washing with distilled water, etching in a solution containing 40% H<sub>2</sub>SO<sub>4</sub> and 30% HNO<sub>3</sub> in a ratio 1:1 (40°C), followed by twice washing in double distilled water. The thickness of the coatings was measured by a non-destructive magnetic-induction method with a caliper of type BB20 of the company BioEviBul.

The coating formation kinetics was evaluated by obtaining of voltammograms, by Wenking (Germany) potentiostat at potential sweep rate of 30 mV s<sup>-1</sup>. The same device was used for the coating depositions, performed at stationary potentiostatic regime.

The corrosion protective properties of the investigated films were evaluated by two electrochemical methods, independent between themselves: Electrochemical Impedance Spectroscopy (EIS) and Linear Sweep Voltammetry (LSV). These measurements were performed by PG-stat Autolab 30 universal potentiostat/ galvanostat, combined with FRA-2 frequency response analyzer. The samples were mounted in standard (ISO 16773)

three-electrode “flat” cells, which provided exposition of 2 cm<sup>2</sup> working surface of the investigated samples in 100 ml of naturally aerated 3.5% NaCl model corrosive medium. Cylindric platinum net was used as counter electrode and “Metrohm” Ag/AgCl/3M KCl electrode served as reference. The impedance spectra and the LSV polarization curves were recorded after defined time intervals: 24, 168, 336, 504 and 672 hours of exposure to the 3.5% NaCl aqueous solution. The spectra were acquired in frequency range between 10 kHz and 10 mHz, distributed into 50 measuring steps at 10 mV, regarding the Open Circuit Potential (OCP). The anodic LSV curves were recorded in Tafel semi-logarithmic coordinates for the newly deposited coatings. The potential interval was selected to be between -270 до 350 mV in respect to Ag/AgCl/3M KCl electrode, at potential scan rate of 5 mV s<sup>-1</sup>, so that the measurements included the corrosion potential ( $E_{corr}$ ) value.

The coating morphology and element composition were defined by Scanning Electron Microscopy (SEM) and Energy Dispersive Spectral Analysis (EDSA), using “Jeol JSM-6390- Oxford Instruments” device. The identification of the crystalline phases was done by X-Ray diffraction analysis (XRD). The respective diffractograms

were acquired by Philips PW 1050, coupled by secondary graphite monochromator. The acquisitions were performed at Cu K $\alpha$  radiation source, at 2 $\theta$  interval, between 10 and 100 angular degrees, at 0.04 $^\circ$  scanning step and 1 s. of exposition per step.

## RESULTS AND DISCUSSIONS

### Deposition kinetics

The film formation kinetics was determined by voltammograms acquisition during deposition of coatings from the electrolytes described in Table 1, at 80  $^\circ\text{C}$  (Fig. 1). The figure shows that the Ni-P deposition proceeds at higher polarization (Fig.1, curve 1) compared to this of the Co-P deposition (Fig.1, curve 2). The current densities reached in the case of Co-P deposition were superior to these of Ni-P and Ni-Co-P. This fact is consequence of both of facilitation of cobalt deposition and porous Co-P film formation. The latter fact was evinced by the morphological analysis, commented in the next paragraph.

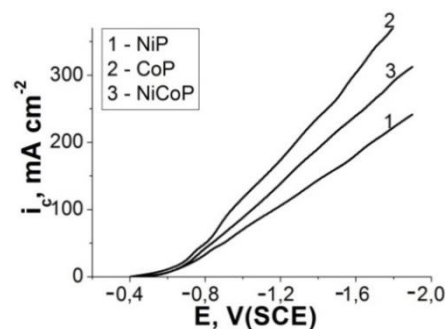
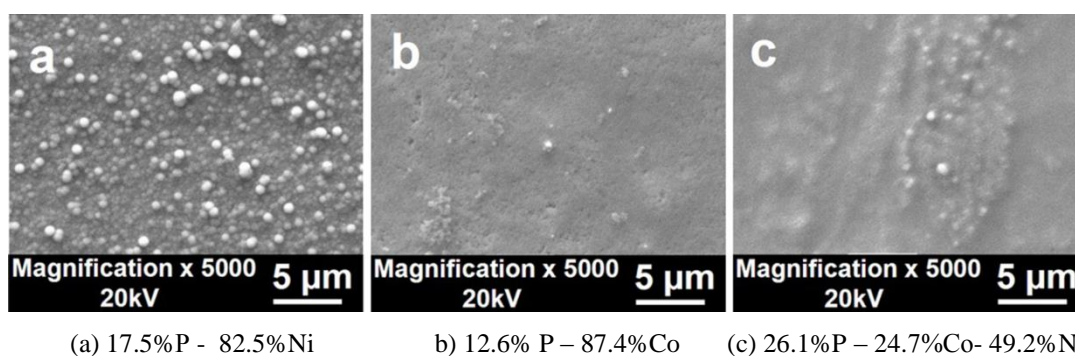


**Fig.1.** Kinetic curves acquired during deposition of Ni-P (1); Co-P (2) and Ni-Co-P (3) coatings at 80 $^\circ\text{C}$ .

### Coating morphology and microstructural analysis

The Scanning Electron Microscopy (SEM) has enabled to obtain data about the morphology of the alloy films (Fig.2) deposited galvanostatically at identical conditions of 65 mAcm $^{-2}$  of current density and 40 min. of electrolysis.



(a) 17.5%P - 82.5%Ni

(b) 12.6% P – 87.4%Co

(c) 26.1%P – 24.7%Co- 49.2%Ni

**Fig. 2.** SEM images of Ni-P (a), Co-P (b) и Ni-Co-P (c) alloyed coatings, deposited at  $i = 65 \text{ mA cm}^{-2}$  for 40 min, from the electrolytes described in Table 1. (the EDSA data are represented in mass.%).

The SEM images in Fig. 2 reveal that all the coatings possess fine grain crystalline configurations. The Ni-P (Fig. 2a) coatings possess a globular structure, composed by spherical crystals with maximal diameter under 1  $\mu\text{m}$ . The Co-P (Fig. 2b) layers are thin (under 1.2  $\mu\text{m}$ , measured with caliper), fine-crystalline and do not cover completely the entire substrate surface. Their incomplete coverage, as it shown by the data of the EIS and LVA methods, commented in the next section, had generally negative effect on their corrosion protective properties. This effect was also confirmed by the polarization curves, commented in the next section. The ternary Ni-Co-P (Fig. 2c) alloy has fine-crystalline structure, with randomly distributed spherical inclusions. The measured thickness of the coatings was about 6  $\mu\text{m}$  for Ni-P and about 4.5  $\mu\text{m}$  for Ni-Co-P.

The morphological and compositional differences among the investigated double and ternary alloy layers have led to distinguishable phase

compositions, as well. It is demonstrated by the XRD patterns, shown in Fig. 3.

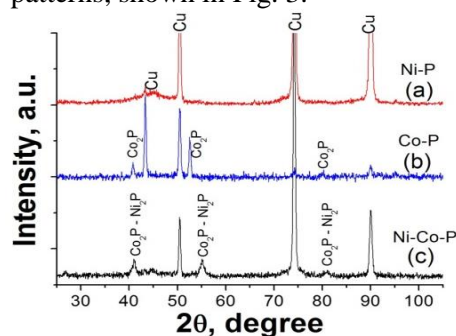


**Fig. 3** X-Ray diffractograms of Ni-P (a), Co-P (b) and Ni-Co-P coatings (c).

The peaks of the copper substrate are distinguishable on all the diffractograms, confirming that the obtained coatings are relatively thin (below 10  $\mu\text{m}$ ). The resulting diffraction peaks are relatively low and wide but with a clearly identifiable location that was used for identification. The estimated average crystallite size of the individual phases

ranged from 35-40 nm. This gave us reason to explain the resulting coating as a nanosized matrix incorporating very few single crystals with an average crystallite size under 1  $\mu\text{m}$ . This finding is also confirmed by the SEM images taken.

The Ni-P coatings are with definitely amorphous structure observable by the diffusion halo (Fig. 3a). In contrary, the Co-P layers (Fig. 3b), deposited at the conditions, and applied in the present research possess homogeneous, polycrystalline structure, consisted by orthorhombic  $\text{Co}_2\text{P}$  phase, regarding the Inorganic Crystal Structure Database (ICSD ref. code: 98-004-3685). The Ni-Co-P coating (Fig. 3c) is the most interesting one. Practically, this coating possesses variable composition consisted by series of solid solution  $\text{Ni}_2\text{P}$  -  $\text{Co}_2\text{P}$  depending on the content of the main elements. However, the diffractions peaks of both  $\text{Ni}_2\text{P}$  and  $\text{Co}_2\text{P}$  phases are indistinguishable due to the overlapping between them. These peaks were determined according to the reference ICSD data values for:  $\text{Co}_2\text{P}$  ref. code: 98-004-3685; and for  $\text{Ni}_2\text{P}$  - ref. code: 98-002-7162, respectively

#### Barrier ability and durability evaluation

The use of two electrochemical methods EIS and LSV, which are independent between themselves, has enabled to evaluate both the barrier ability and durability of the investigated Ni-P, Co-P and Ni-Co-P alloyed coatings, deposited on copper substrates. These corrosion protective abilities were additionally determined for Ni-Co alloy film, deposited from the same electrolyte (Table 1), but without phosphorous containing ingredients. This coating was deposited at the same conditions ( $I = 65 \text{ mAcm}^{-2}$  for 40 min.), as the rest ones.

The EIS and LSV electrochemical measurements were performed for extended period – from 24 to 672 hours of exposure to 3.5% NaCl model corrosive medium. Figure 4 represents the Bode and Nyquist plots of the EIS spectra, acquired respectively for: Ni-P (Fig. 4a), Co-P (Fig. 4b), Ni-Co-P (Fig. 4c) and Ni-Co (Fig. 4d), during the entire 672 hours of exposure.

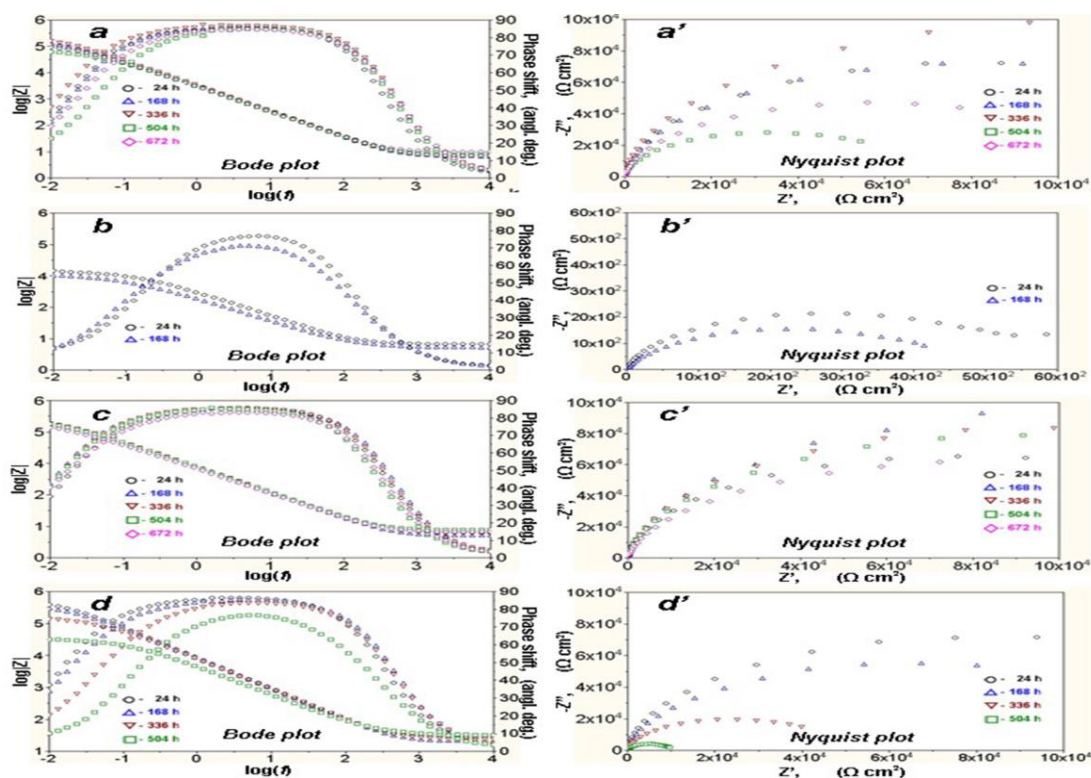


**Fig. 4.** EIS spectra recorded after different exposure times for: Ni-P (a), Co-P (b), Ni-Co-P (c) and NiCo - (d), represented in Bode (left side) and Nyquist (right side) plots.

On the basis of the comparizon among the Bode plots of the impedance spectra in Fig. 4, recorded for each one of the investigated samples it could be inferred that the Ni-P and Ni-Co-P compositions

possess remarkably higher barrier ability than Co-P and Ni-Co ones. The entire orders of magnitude higher impedance modulus at 0.01 Hz, equal to  $|Z| = 10^{5.5}$  and  $10^5 \Omega \text{ cm}^2$  for Ni-P and Ni-Co-P, compared

to  $|Z| = 10^{3.5} \Omega \text{ cm}^2$  for Co-P, is indication for the rather superior barrier ability of the former Ni-containing compositions. The Ni-Co coating occupies an intermediate position with  $|Z| = 10^{4.5} \div 10^5 \Omega \text{ cm}^2$ .

The phase shift ( $\varphi$ ) between the sinusoids of the applied potential and the resulting current density for the Ni-P, Ni-Co-P and Ni-Co reaches  $90^\circ$ , corresponding to almost pure capacitance, whereas for Co-P film, it decreases down to  $\varphi \sim 70^\circ$ . This fact is an evidence for the almost pure capacitive character of the electric double layer (EDL) between the model corrosive medium and the Ni-P, Ni-Co-P and Ni-Co coatings, being undoubted evidence for their nano-sized structures. The exponent „n“ values in their cases tend to unit (i.e. 100%) (Table 2). These facts conceive that the EDL resembles the behaviour of almost ideal flat capacitor and consequently, the Ni-P, Ni-Co-P and Ni-Co coatings are smooth and with high crystal distribution homogeneity. The indistinguishable deviations between the real EIS spectra recorded and the respective equivalent circuit serves as an additional evidence for the coating uniformity of the Ni-P, Ni-Co-P and Ni-Co coatings

The Nyquist coordinates presentation of the EIS spectra renders even clearer image for the differences for each specimen and the deterioration of their barrier ability after the respective exposure periods. The highest real (corresponding to the Ohmic resistance), and imaginary (related to the capacitive resistance) impedance values, acquired after 24 hour of exposure [19] belong to the Ni-P coating, followed subsequently by Ni-Co, Ni-Co-P and Co-P. The fitting of the real electrochemical impedance spectra of the investigated samples to spectra of suitable equivalent circuits has allowed defining all the resistances and capacitances occurring in the electrolyte/coating/substrate system. In the present case, the selected equivalent circuit comprised 3.5% NaCl, electrolyte resistance  $R_{el}$ , electric charge transfer resistance  $R_{ct}$  (including all the cathodic and anodic reactions of the corrosion process), and Constant Phase element CPE (i.e. pseudocapitance) of the electric double layer on the interface between the coating surface and the 3.5% NaCl solution. The equivalent circuit is shown in Figure 5.

The values determined by the quantitative analysis of the impedance spectra, recorded after 24 hours of exposition (Table 2) reveal that the highest barrier ability is owed by Ni-P and Ni-Co alloys, followed by Ni-Co-P composition, corresponding to

$R_{ct} = 300.80, 295.00$  and  $271.40 \text{ k}\Omega \text{ cm}^2$ , respectively. For comparison, the  $R_{ct}$  obtained from the Co-P film is by entire order of magnitude lower, reaching  $10.82 \text{ k}\Omega \text{ cm}^2$ , which results from the incomplete coverage of the surface.

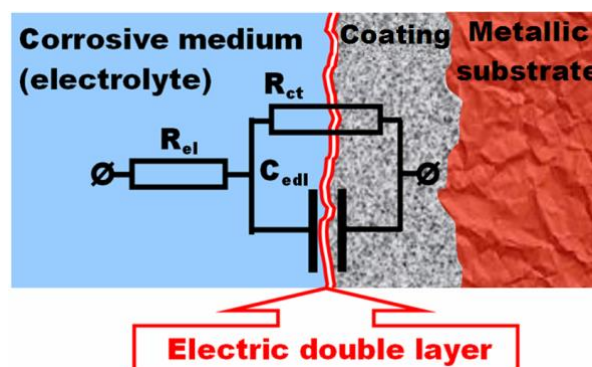


**Fig. 5.** Equivalent circuit used for EIS data fitting:  $R_{el}$  – MCM electrolyte resistance;  $C_{edl}$  – electric double layer capacitance;  $R_{ct}$  – charge transfer reactions resistance

The comparison of the spectra for Ni-P, Ni-Co-P and Ni-Co coatings, especially in Nyquist coordinates (Fig. 4 a, c, d)) and the  $R_{ct}$  data summarized in Table 2 for the respective exposure periods shows that the ternary Ni-Co-P coating possesses the highest durability of the barrier properties, compared to these of Ni-P and Ni-Co coatings. Indeed, both the real and the imaginary impedance components recorded for the entire 672 hours of exposure for Ni-P and especially for Ni-Co decrease more rapidly than for the Ni-Co-P composition. From the  $R_{ct}$  data in Table 2, it can be seen that  $R_{ct}$  of Ni-Co-P decreases to a lesser degree than for the Ni-P coating. On the other hand, the most remarkable barrier properties deterioration belongs to Ni-Co and Co-P coatings. The former, Ni-Co reaches very low  $R_{ct}$  value, equal to only  $R_{ct} = 19.36 \text{ k}\Omega \text{ cm}^2$  (Table 2), whereas the latter Co-P layer was completely destroyed after the initial 168 hours of exposure. Negligible  $R_{ct}$  increase was detected for the Ni-Co-P, and Ni-P compositions after respectively the 168<sup>th</sup> and the 336<sup>th</sup> hour of exposure, instead of the expected decrease. It could be explained assuming corrosion products accumulation, which disturbs the access of the corrosive species towards the coating surfaces [10]. Another explanation for the observed effect is the reported by some authors [9, 10] increase of the phosphorus content of the coating by increasing its thickness. This fact is reflected so in the impedance spectra shapes, so in the respective  $R_{ct}$  values.

**Table 2.** Values of the electrolyte Ohmic resistance  $R_{el}$ , the electric double layer pseudocapacitance  $CPE_{edl}$  and the charge transfer resistance  $R_{ct}$  acquired by the impedance modeling for Ni-P, Co-P, Ni-Co-P and Ni-Co coatings.

<b>SAMPLE: NiP (A)</b>									
Hours of exposure	<b>Rel</b> [ $\Omega.cm^2$ ]		<b>CPE<sub>edl</sub> (x10<sup>-5</sup>)</b> [ $s^n.\Omega^{-1}.cm^{-2}$ ]		<b>n</b> [-]		<b>R<sub>ct</sub>(x10<sup>3</sup>)</b> [ $\Omega.cm^2$ ]		
	v	E %	v	E %	v	E %	v	E %	
24h	19.50	1.07	2.73	0.82	0.96	0.19	300.80		2.13
168h	13.68	0.83	2.66	0.60	0.96	0.14	302.20		1.56
336h	13.44	0.77	2.73	0.54	0.96	0.12	404.40		1.71
504h	14.38	1.43	12.76	1.17	0.95	0.26	121.00		2.04
672h	13.08	1.09	12.82	0.81	0.94	0.19	200.20		1.88

<b>SAMPLE: CoP (B)</b>									
Hours of exposure	<b>Rel</b> [ $\Omega.cm^2$ ]		<b>CPE<sub>edl</sub> (x10<sup>-5</sup>)</b> [ $s^n.\Omega^{-1}.cm^{-2}$ ]		<b>n</b> [-]		<b>R<sub>ct</sub>(x10<sup>3</sup>)</b> [ $\Omega.cm^2$ ]		
	v	E %	v	E %	v	E %	v	E %	
24h	16.06	1.43	11.57	1.78	0.88	0.47	10.82		1.88
168h	7.51	0.99	20.78	1.14	0.84	0.33	8.52		1.45

<b>SAMPLE: NiCoP (C)</b>									
Hours of exposure	<b>Rel</b> [ $\Omega.cm^2$ ]		<b>CPE<sub>edl</sub> (x10<sup>-6</sup>)</b> [ $s^n.\Omega^{-1}.cm^{-2}$ ]		<b>n</b> [-]		<b>R<sub>ct</sub>(x10<sup>3</sup>)</b> [ $\Omega.cm^2$ ]		
	v	E %	v	E %	v	E %	v	E %	
24h	17.16	0.91	31.34	0.69	0.95	0.16	271.40		1.87
168h	14.28	0.82	30.71	0.57	0.95	0.13	390.00		1.97
336h	15.96	0.73	31.45	0.53	0.95	0.13	346.00		1.69
504h	21.80	0.87	32.84	0.67	0.95	0.17	323.60		2.11
672h	18.74	1.28	37.47	0.97	0.93	0.24	246.80		2.85

<b>SAMPLE: NiCo (D)</b>									
Hours of exposure	<b>Rel</b> [ $\Omega.cm^2$ ]		<b>CPE<sub>edl</sub> (x10<sup>-6</sup>)</b> [ $s^n.\Omega^{-1}.cm^{-2}$ ]		<b>n</b> [-]		<b>R<sub>ct</sub>(x10<sup>3</sup>)</b> [ $\Omega.cm^2$ ]		
	v	E %	v	E %	v	E %	v	E %	
24h	16.78	0.73	33.60	0.56	0.96	0.13	295.00		1.65
168h	13.32	1.15	33.97	0.85	0.95	0.20	230.40		2.18
336h	14.10	1.27	40.24	1.07	0.93	0.25	86.60		1.81
504h	19.90	0.75	74.65	0.83	0.87	0.21	19.36		0.94
672h	-	-	-	-	-	-	-		-

The application of LSV as an electrochemical method, alternative to EIS and the further Tafel slope analysis data have enabled to acquire supplemental data about the corrosion protective abilities of the films on the basis of the corrosion potential  $E_{corr}$  and the polarization resistance  $R_p$  values (Table 3).

The anodic polarization curve shapes (Fig. 6, a-d) and the data in Table 3 confirm the statement for the higher barrier ability of the Ni-P (Fig. 6a) and Ni-Co-P (Fig. 6c), in comparison to this of the Ni-Co (Fig. 6d) and Co-P (Fig. 6b).

**Table 3.** Data for the corrosion potential,  $E_{corr}$ , [mV] vs. Ag/AgCl and the polarization resistance  $R_p$ , [ $k\Omega cm^2$ ] determined by the anodic (Tafel) polarization curves for different periods of exposure of the investigated samples to the model corrosive medium

Exposure time	Ni-P (A)		Co-P (B)		Ni-Co-P (C)		Ni-Co (D)	
	$E_{corr}$ , mV	$R_p$ , $k\Omega cm^2$	$E_{corr}$ , mV	$R_p$ , $k\Omega cm^2$	$E_{corr}$ , mV	$R_p$ , $\Omega cm^2$	$E_{corr}$ , mV	$R_p$ , $k\Omega cm^2$
24 h	-266	147.28	-208.0	10.24	-246.0	231.00	-223	372.00
168 h	-258	302.60	-189.0	9.30	-321.0	378.80	-199	224.40
336 h	-257	289.40	corrosion	corrosion	-213.0	601.00	-215	80.56
504 h	-180	101.48	corrosion	corrosion	-186.0	223.20	-169	16.30
672 h	-230	194.42	corrosion	corrosion	-173.0	267.80	corrosion	corrosion

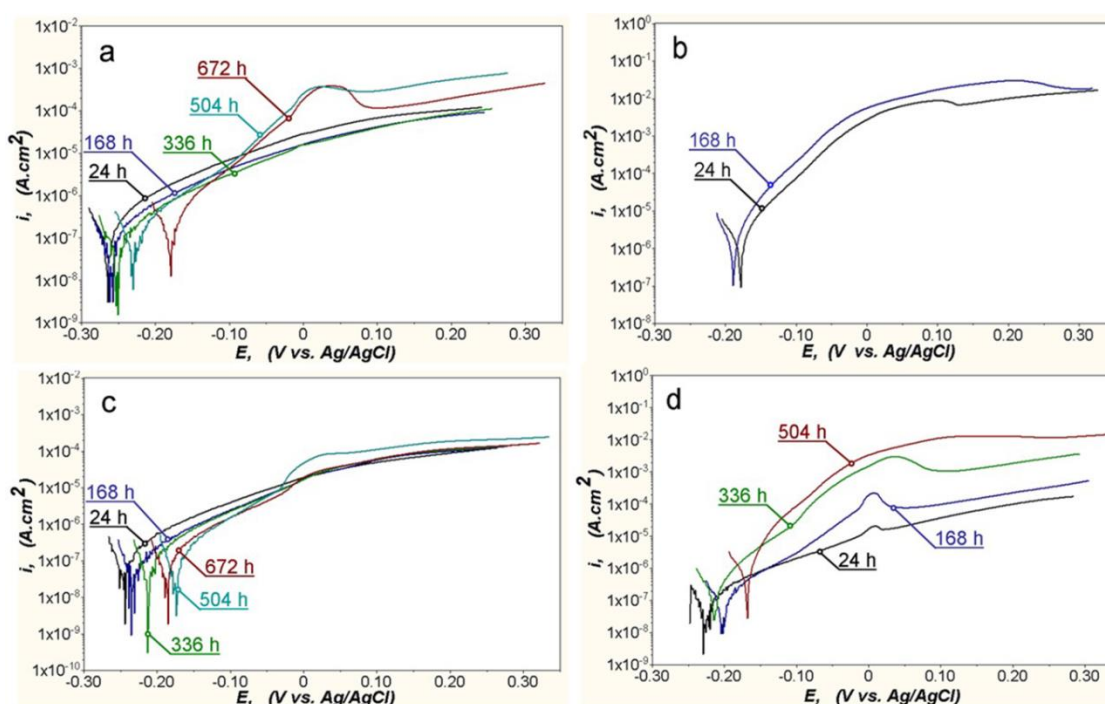


**Fig. 6.** Anodic polarization curves, recorded during the entire 672 hours of exposure for Ni-P (a), Co-P (b), Ni-Co-P (c) and Ni-Co (d) coatings

Weak current density change within the anodic polarization for Ni-P and Ni-Co-P was observed until the 336<sup>th</sup> hour of exposition. Afterwards, at 504 hours of exposure, the respective curves change sharply their shape. The dissolution current rises and passes through a maximum at about 0.025 V. Such current increase was observed for the Ni-Co composition after 168 hours of exposure. The occurrence of the observed maxima in the anodic curves can be explained by corrosion products accumulation. In the case of the Ni-P film, these maxima are more sharp (Fig. 6a), due probably to the denser structure of the respective corrosion products, compared to this of the Ni-Co-P coating (Фиг. 6c). Literature data exist [20, 21] which report that the active Ni-P dissolution leads to phosphorous heaping, as a result of selective Ni-dissolution during anodic polarization. Simultaneously,  $Ni_3(PO_4)_2$  film

formation proceeds, contributing as a barrier against further dissolution. That is why, the Ni-Co-P ternary film has revealed the highest  $R_p$  values during the entire exposure period (Table 3), compared to Ni-P and especially to Co-P. In the case of Ni-Co coating, the  $R_p$  were high only at the initial 24 hours of exposure, and afterwards, these values decrease sharply.

The  $R_p$  values measured for all the investigated compositions (Table 3) follow the same trend, as the respective  $R_{ct}$  (Table 2), obtained by the impedance modeling. Because the  $R_p$  includes both  $R_{ct}$  and the oxide layer resistance  $R_{oxy}$  (i.e.  $R_p \approx R_{ct} + R_{oxy}$ ) [22], it could be assumed that the anomalous  $R_p$  rise for the ternary Ni-Co-P coating (Table 3) after 336 hours of exposure, up to 601.00  $k\Omega cm^2$  is a result of both increasing the phosphorus content with the thickness of the film [9,10] and the formation of an oxidation film.

## CONCLUSIONS

The Ni-P, Co-P and Ni-Co-P alloy films, deposited at identical conditions at galvanostatic regime, possess different crystal structure, phase composition and corrosion resistance. It was found:

(1) The estimated from the XRD patterns average crystallite size of the individual phases for all coatings ranged from 35 to 40 nm, i.e. the resulting coatings are nanosized matrix incorporating very few single crystals with an average crystallite size under 1  $\mu\text{m}$ .

(2) The Ni-P coatings (17.5% P - 82.5%Ni) are typically amorphous and possess a globular structure.

(3) The Co-P layers (12.6% P – 87.4%Co) are thin (under 1.2  $\mu\text{m}$ ) and do not cover completely the entire substrate surface. They consist of orthorhombic Co<sub>2</sub>P phase.

(4) The ternary Ni-Co-P alloy (26.1%P – 24.7%Co- 49.2%Ni) possesses variable composition consisted by series of solid solution Ni<sub>2</sub>P - Co<sub>2</sub>P.

(5) The quantitative analysis of the impedance spectra, together with the respective anodic LSV polarization curves have revealed that the highest barrier ability and corrosion resistance belong to the Ni-Co-P three-component layer.

**Acknowledgements:** The authors acknowledge the Scientific Research Section to UCTM – Sofia for the financial support via Project 2FHN\_K\_I – 2017 (internal №11642)

## REFERENCES

1. M. Crobù, A. Scorciapino, B. Elsener, A. Rossi, *Electrochim. Acta*, **53**, 3364 (2008)
2. P. Cojocaru, L. Magagnin, E. Gomez, E. Valles, *J. Alloys Compd.*, **503**, 454 (2010).
3. R.K. Shervedani, A. Lasia, *J. Electrochem. Soc.*, **144**, 511(1997).
4. N.M. Alanazi, A.M. El-Sherik, S. H. Alamar and Sh. Shen, *Int. J. Electrochem. Science*, **8**, 10350 (2013).
5. J.L. Crea, *Surf. Eng.*, **26**, 149 (2010).
6. H. Jung, A. Ajfanazi, *Electrochim. Acta*, **51**, 1806 (2006).
7. Lucas I., L.Perez, C. Aroca, P. Sanchez, E. Lopez, M. C. Sanchez, *J. Magn. & Magnet. Mater.*, **290-291**, 1513 (2005).
8. G. Hibbard, K.T.Aust, G. Palumbo, *U. Erb, Scripta Mater.*, **44**, 513 (2001).
9. C. Ma, S. Wang, F. C. Walsh, review, Transactions of the IME, *Internat. J. Surf. Eng. Coat.*, **93**, 275 (2015).
10. M.M.V. Parente, O.R. Mattos, S.L. Diaz, P.L. Neto, F.J.F. Miranda, *J. Appl. Electrochem.*, **31**, 677 (2001).
11. R.A. Prado, D. Facchini, N. Mahalanobis, F. Gonzalez, G. Palumbo, 2009 DoD Corrosion Conference, NAVAIR Public Release 09-776, 1-13 (2009).
12. C. Ma, S. Wang, F. C. Walsh, *Transactions of the IME*, **93**, 1, 8 (2015).
13. K. S. Lew, M. Raja, S. Thanikaikarasan, T. Kim, Y. D. Kim, T. Mahalingam, *Mater. Chem. Phys.*, **112**, 249 (2008).
14. J. Ahmad, K. Asami, A. Takeuchi, D.V. Louzquine, A. Inoue, *Materials Transactions*, **44**, 911 (2003).
15. S. S. Djokic, *J. Electrochem. Soc.*, **146**, 1824 (1999).
16. T. Morikawa, T. Nakade, M. Yokoi, Y. Fukumoto and C. Iwakura, *Electrochim. Acta*, **42**, 115 (1997).
17. R. Raicheff, V. Zapryanova, *J. Mater. Sci. Lett.*, **19**, 3 (2000).
18. F. Zhaoeng, *Trans. Nonferrous Met. Soc. China*, **7**, 148 (1997).
19. B.A. Boukamp, *Solid State Ionics*, **18-19**, 136 (1986).
20. H. Habazaki, S.Q. Ding, A. Kawashima, K. Asami, K. Hashimoto, A. Inoue, T. Masumoto, *Corros. Sci.*, **29**, 1319 (1989).
21. S.J. Splinter, R. Rofagha, N. S. McIntyre, U. Erb, *Surf. Interface Anal.*, **24**, 181 (1996).
22. E.A. Matter, S. Kozhukharov, M. Machkova, V. Kozhukharov, *Mater. Corros.*, **64**, 408 (2013).



## СТРУКТУРА И КОРОЗИОННА УСТОЙЧИВОСТ НА Ni-P, Co-P И Ni-Co-P СПЛАВНИ ПОКРИТИЯ

Катя Н. Игнатова<sup>1</sup>, Стефан В. Кожухаров<sup>1</sup>, Георги В. Авдеев<sup>2</sup>, ИскраАт. Пироева<sup>1</sup>

<sup>1</sup>Химикотехнологичен и металургичен университет, бул. "Климент Охридски" 8, 1756 София, България

<sup>2</sup>Институт по физикохимия „Ростислав Каишев“, Българска академия на науките, ул. "Акад. Георги Бончев" бул. 11, 1113 София, България

Постъпила на 21 август, 2017 г.; приета на 07ноември, 2017 г.

(Резюме)

Настоящата статия докладва резултатите от систематичното охарактеризиране на морфологията, фазовия състав, бариерната способност и корозионната устойчивост на Ni-P, Co-P и Ni-Co P покрития върху мед. Изследваните покрития са отлагани галваностатично при съпоставими условия от сулфатно-хлориден електролит с рН = 2 при 80°C. SEM анализът установи, че получените покрития са наноразмерни с фино кристална структура, потвърдена и от резултатите на XRD анализа. Резултатите от XRD анализа показаха, че Ni-P сплавни покрития са с типично аморфна структура, докато Co-P покрития са с хомогенна поликристална структура, съставена от орторомбична Co<sub>2</sub>P фаза. Ni-Co- P покрития са с различен фазов състав в зависимост от съдържанието на основните елементи, представляващ серия от твърди разтвори Ni<sub>2</sub>P –Co<sub>2</sub>P. Данните от методите на импедансната спектроскопия (EIS) и на линейната волтаперометрия (LSV) за бариерната способност и корозионната устойчивост на изследваните покрития са в пълна корелация. Количествените данни от двата метода, получени за интервал на престояване на покритията от 24 до 672 часа в 3.5% NaCl показаха, че най-добри защитни характеристики има тройната сплав Ni-Co-P. Освен това Ni-Co-P и Ni-P сплавни покрития запазват бариерната си способност за цялото време от 672 h на престояване в разтвора. Co-P покрития напълно се разрушават след 168 часа престояване в моделната корозионна среда.

**Ключовидуми:** Ni-Co- P, сплавни покрития, морфология, фазов състав, корозия, импедансен метод